Supporting Information

Graphene Oxide Dispersions: Tuning Rheology to Enable Fabrication

Sina Naficy[‡ a], Rouhollah Jalili[‡ a], Seyed Hamed Aboutalebi[‡b], Robert A. Gorkin III [a], Konstantin Konstantinov[b], Peter C Innis [a], Geoffrey M. Spinks [a], Philippe Poulin[c] and Gordon G. Wallace [a] *

[a] *Intelligent Polymer Research Institute and ARC Centre of Excellence for Electromaterials Science AIIM Facility, Innovation Campus, University of Wollongong, North Wollongong, NSW 2522, Australia*
[b] *Institute for Superconducting and Electronic Materials, AIIM Facility, Innovation Campus, University of Wollongong, North Wollongong, NSW 2522, Australia*
[c] *Centre de Recherche Paul Pascal, Université Bordeaux I, UPR CNRS 8641, France*
Email: gwallace@uow.edu.au

This supplementary information contains the following:

Experimental

Graphene oxide dispersions were prepared following previously described method [2]. The resultant large GO sheets were dispersed in Milli Q water at various concentrations ranging from 0.05 mg ml^{-1} to 13.3 mg ml^{-1}. Rheological measurements were performed using a TA rheometer (AR G2) with a cone-plate geometry (60 mm, 2°). After loading the rheometer with GO dispersions (2.1 ml), samples were allowed to equilibrate for another 4 hrs at the experimental temperature (25 °C) to eliminate any flow history before the course of the experiment. Electrospraying of GO dispersions on PET substrate was performed using a MECC-NANON machine when the applied voltage was set to 20kV. Inkjet printing of LC GO dispersions of GO on paper and glass substrates was performed using a custom Pixdro LP50 system (Roth & Rau, Netherlands), using Spectra printheads (S-class SL-128AA, Dimatix, USA) and appropriate settings. Wet spinning and dry spinning were performed using a custom made spinning system described previously [2]. Spray coating of GO thin films on glass substrate was carried out using a Flexicoat R&D ultrasonic spray coating system (Sono-Tek, USA)

using a 60kHz nozzle with a feed rate of 0.2 ml min^{-1} and amplitude of 2.5. Extrusion printing of LC GO gels was carried out using a 3D-Bioplotter (EnvisionTEC, Germany).

Rheological properties of various concentrations of GO dispersion were investigated using a TA rheomotere (AR G2). A cone-plate geometry (60 mm, 2^{o}) was used to perform experiments. All samples were made freshly from two GO stock solutions: 4.5 mg ml^{-1} and 13.35 mg ml^{-1}. Samples were prepared by diluting the above solutions with deionized water, one day prior to the test. Different volume ratios of GO stock solution and distilled water were mixed thoroughly and then allowed to rest overnight before the each rheological test. After loading the rheometer with GO dispersion samples (2.1 ml) with various GO concentration, samples were allowed to rest in the final position for another 4 hrs at the experimental temperature (25 ^{o}C), in order to eliminate the any viscoelastic history. No prestressing condition was applied to prevent ordering in the samples. A solvent trap filled with distilled water was used to prevent GO samples of losing water over the course of long experiments.

The relaxation dynamic of GO dispersions was studied by measuring the storage modulus and loss modulus of GO dispersions with various GO concentration as a function of frequency at a constant strain amplitude of 0.01. This strain amplitude was chosen to prevent samples of going under large deformations. In the preliminary shear experiments it was shown that strains larger than 0.01 could result in a structure change. Consequently, the larger deformations could mask the relaxation behaviour of GO dispersion. The concentration of GO in the GO dispersions ranged from as low as 0.05 mg ml^{-1} ($\phi \cong 2.27\times10^{-5}$) up to 13.35 mg ml^{-1} ($\phi \cong 6.07\times10^{-3}$). The range of GO sheet volume concentrations used in this study is considerably wider than similar studies for SWNT dispersions [1].

The zero shear viscosity was measured using a simple shear experiment in which shear rate was ramped from 10^{-3} s^{-1} up to 100 s^{-1}. The viscosity measured at shear rates less than 0.01 s^{-1} was not stable for GO dispersions with GO concentration less than ~ 0.1 mg ml^{-1}, as a result the lowest possible shear rate in which viscosity could be reported for all dispersions is 0.01 s^{-1}.

Supplementary Discussion

The measured storage and loss moduli are presented in Fig. S2 as a function of angular frequency for a series of GO concentration. Both elastic and viscose elements of GO dispersions were high enough to enable measurements even at concentrations as low as 0.05 mg ml^{-1}. In dilute GO concentrations, G" slightly dominates the viscoelastic behaviour of dispersions over the entire frequency range. As GO concentration increases both G' and G" begin to become more frequency-independent over longer range of frequencies. Eventually at concentrations as high as 4.5 mg ml^{-1} G' is the dominant part over the entire range of frequency (experimental time of 10^{-3} to 50 sec^{-1}). The dominancy of G' over G" at lower frequency ranges can be interpreted as a measure of those structural relaxation times of the GO dispersion system that are not accessible at the corresponding experimental time scales in which the measurement is carried out. At medium GO concentration, shorter relaxation times originated from individual GO domains fall within the experimental time scale while longer relaxation times which require long range collaborative relaxation between GO domains are not seen even at very low frequencies. As GO concentrations increases even the shorter relaxation times are now becoming inaccessible within the experimental time scales performed here. The measured storage modulus for GO dispersions is found to be considerably higher than the storage modulus of SWNT suspensions with similar concentrations. For example the measured G' for the 13.35 mg ml^{-1} GO dispersion ($\phi \cong 6.07\times10^{-3}$) is ~ 417 Pa, while the G' of a SWNT suspension with SWNT concentration around 6×10^{-3} is ~ 60 Pa [1]. Of note, the aspect ratio of SWNTs used in ref 1 is ~ 165, while the aspect ratio of GO sheets used in our study (~45000) is much larger (Fig. S1).

From Fig. S2, it seems that the GO dispersions exhibit a diverse range of rheological properties, ranging from a simple viscoelastic fluid to a soft glassy viscoelastic fluid to a gel-like material. This diversity in the rheological properties of a single material can be a key reason for possible widespread technological utilities. Control over the rheology may be achieved by adjusting the volume fraction of GO particles. Similar trend was reported for MWNT suspensions (Fig. 5b in ref [1]).

The storage modulus of GO dispersions (where G'>G") was interpreted in terms of the percolation theory. The storage modulus of those GO dispersions in which G'>G" was treated as a constant

plateau storage modulus G'_o where G'_o=G' at frequency 0.01 sec^{-1}. Assuming a percolation behaviour for storage modulus as a function of GO concentration, G'_o was plotted against GO volume fraction: $G'_o \sim (\phi - \phi^*)^v$, and ϕ^* and v were found to be, respectivey, ~$2.3\times10^{-4} \pm 0.7\times10^{-4}$ and 2.75 ± 0.15. The percolation volume fraction estimated here was one order of magnitude lower than that of SWNT suspensions reported before (2.6×10^{-3}). The predicted *geometrical* volume fraction percolation threshold for randomly oriented overlapping plates with an aspect ratio of ~ 30000 is ~ 3.1×10^{-5} to 4.2×10^{-5} .

The estimated exponent we obtained here (2.75± 0.15) is higher than the exponent obtained in for SWNTs (2.3 ±0.1), and falls in the range of 2.1 – 3.2 which was observed before for gelation threshold of some polymer systems.[3] Our estimated exponent is close to the numerical results obtained for the Young's modulus of a percolating system in a 2D disk system (3.2±0.4) [4].

The storage modulus can also be interpreted as a function of frequency using this simplified equation $G'(\omega) \approx G'_o \omega^n$, where G'_o is the plateau storage modulus, ω is the frequency and n is a constant. More generalized Maxwell model composed of a series of parallel dashpots and springs is in the form of: $G' = \sum_{i:1}^{n} G_i \frac{(\lambda_i \omega)^2}{1+(\lambda_i \omega)^2}$, where n is the number of elements, G_i is the spring constant of the ith element , λ_i is the relaxation time of the ith Maxwell element and is related to the dashpot viscosity η_i and spring constant of that element according to $\lambda_i = \frac{\eta_i}{G_i}$. n is ~ 2 for a Maxwellian (linear viscoelastic) fluid at low frequencies. When $n \rightarrow 0$, the elastic modulus becomes independent of the experimental time scale in which the measurements are performed. Fig. S3 represents n as a function of GO volume fraction for frequencies where G' follows power-law behaviour. As can be seen, when GO concentration increases above 0.5 mg ml^{-1} (2.2×10^{-4}) n begins to suddenly drop one order of magnitude down to 0.03, meaning that the storage modulus was not very dependent to the frequency (as can be seen in Fig. S2 as well). This frequency dependence of the moduli can be well described in the light of the rheology of soft glassy materials [5]. This framework suggests that there was a generic presence of slow glassy dynamics in the viscoelastic behaviour of a wide range of soft materials (e.g.

clay slurries, paints, microgels, pastes, colloidal glasses, and dense emulsions) in which G'>G" down to very low frequencies (10^{-3} – 1 Hz).

The effect of strain amplitude on the structure of GO dispersion is revealed through G' and G" measurements at 0.01 Hz as a function of strain (Fig. 3). Unlike some of the cross-linked biopolymer networks [6] no strain hardening was observed here. At the same time, unlike swollen rubbers and hydrogels in which the response is mainly elastic and linear the GO dispersion exhibits a non-linear response, suggesting that the structural network of GO sheets is not permanently elastic and can go through a yield point, that is when G'=G". A fluidization region can be seen before the yield point was reached where G" slightly rises before crossing the decaying G'. This Non-linear viscoelastic phenomenon has been reported previously for many soft material systems [4,7]. A flow behaviour similar to that of entangled polymeric fluids [8] was also observed here under a continuous simple shear in which a yield stress appeared slightly after start-up.

Assuming a linear behaviour before yielding, the yield point can define a maximal elastic energy stored in the system before reaching the yield point. Interestingly, the viscoelastic behaviour of GO dispersion system as a function of GO volume fraction can be divided into 3 different regimes (Fig. S4). When GO volume fraction was less than ~ 3×10^{-4}, no significant yielding was observed. As GO volume fraction increases above 3×10^{-4} up to 3×10^{-3} yield strain increases with GO volume fraction. Similar trends were reported before for "soft glassy" particle with *repulsive* interactions [9]. By increasing the GO volume fraction beyond 3×10^{-3} yield strain starts to decline slowly. A similar behaviour was reported before for SWNT suspensions [1].

Fig. 4 shows that the viscosity exhibits a sudden drop as GO concentration increases to 2.2×10^{-4}. The viscosity keeps increasing with GO concentration after this maxima up to ~ 100 Pa s, then levels off when GO concentration reaches to 3.0×10^{-3} and again begins to increase considerably as GO concentration increases further (~ 650 Pa s at 6.1×10^{-3}). For SWNT suspensions in superacid [10] a similar phase transition was reported for SWNT concentrations 0.04 – 0.05, where viscosity dropped from ~ 1000 Pa s at ~ 0.04 to ~ 300 Pa s at ~ 0.05. To reach the 650 Pa s in LC phase, the required

volume fraction of SWNT in superacid was ~ 0.06 – 0.08 [9], compared to only ~ 0.006 GO in water to obtain the same viscosity with LC properties.

The intrinsic viscosity of the GOs was calculated using the linear fit equation in Fig. S5. The intrinsic viscosity is the zero concentration limiting value of the reduced specific viscosity and is a ameasure of the characteristic function of a single molecule in the solution. The calculated intrinsic viscosity for a GO sheet was ~ 198 dL g^{-1}, which is greater than that of SWNTs (57 dL g^{-1}, L=0.47 – 1.5 μm), xanthan molecules (71 dL g^{-1}, L=2.8 μm), poly(benzobisoxazole) (50 dL g^{-1}, L=390 nm), and poly(*p*-benzamide) (12.5 dL g^{-1}, L=400 nm) [10,11]. Using Kuhn and Kuhn relationship for disks [12] the calculated aspect ratio is ~ 29000 for a GO sheet. The estimated aspect ratio for the GO sheet is ~ 22400 – 44800 [13].

Supplementary Figures and Legends

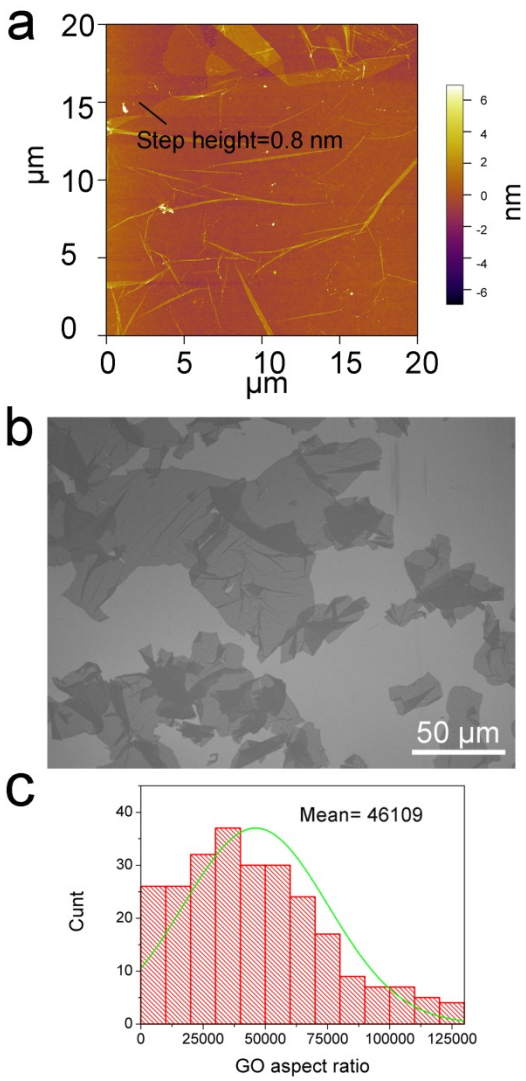

Fig. S1. **a**) Representative AFM image of an ultra large GO sheet. The marked line in the AFM image shows the place which we measured the thickness of the GO sheet confirming the presences of a monolayer of GO with apparent thickness of 0.8 nm. Also, AFM studies show that GO dispersions predominantly contained monolayer of GO sheets. **b**) SEM image of GO sheets present in as-prepared GO dispersions contain ultra large GO sheets. Both AFM and SEM images present highly wrinkled nature of the GO sheets which confirms flexibility. **c**) The corresponding distribution of the aspect ratio of GO sheets.

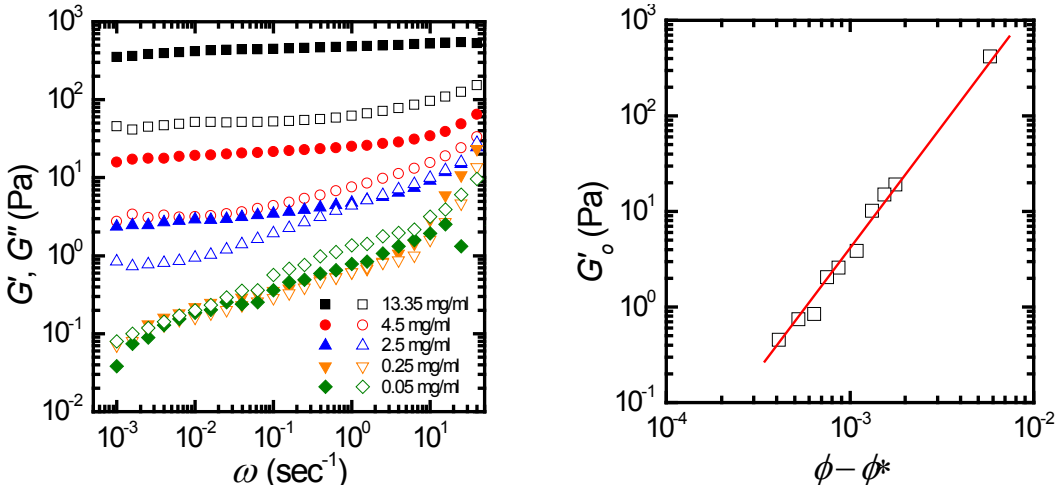

Fig. S2. (A) Storage and loss moduli of GO suspensions with varying concentration: 13.35 mg ml^{-1}, 4.5 mg ml^{-1}, 2.5 mg ml^{-1}, 0.25 mg ml^{-1} and 0.05 mg ml^{-1}. (B) Storage modulus of GO suspension at 0.01 Hz vs $(\phi - \phi^*)$, where ϕ is GO volume fraction. $G_o' \sim (\phi - \phi^*)^{\upsilon}$: $\phi^* \cong 2.3\times10^{-4} \pm 0.7\times10^{-4}$; $\upsilon \cong 2.75 \pm 0.15$.

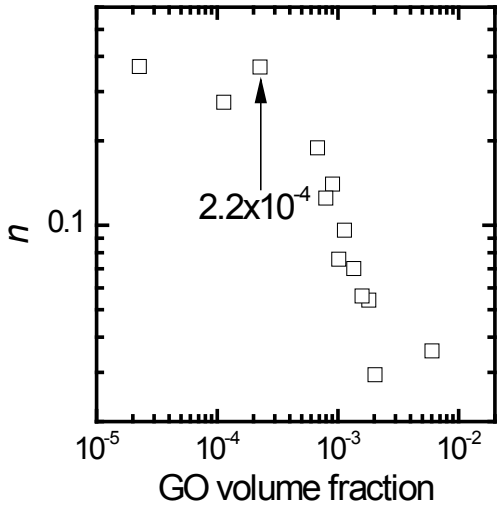

Fig. S3. n as in $G'(\omega) \approx G'_o\omega^n$ vs GO volume fraction, where ω is the frequency. n is ~ 2 for a Maxwellian (linear viscoelastic) fluid. The drop in n indicates the dominance of storage modulus over a wide range of frequency in which storage modulus remains almost independent of frequency. The sudden decay in n was observed when GO volume fraction exceeds beyond 2.2×10^{-4} (0.5 mg ml^{-1}).

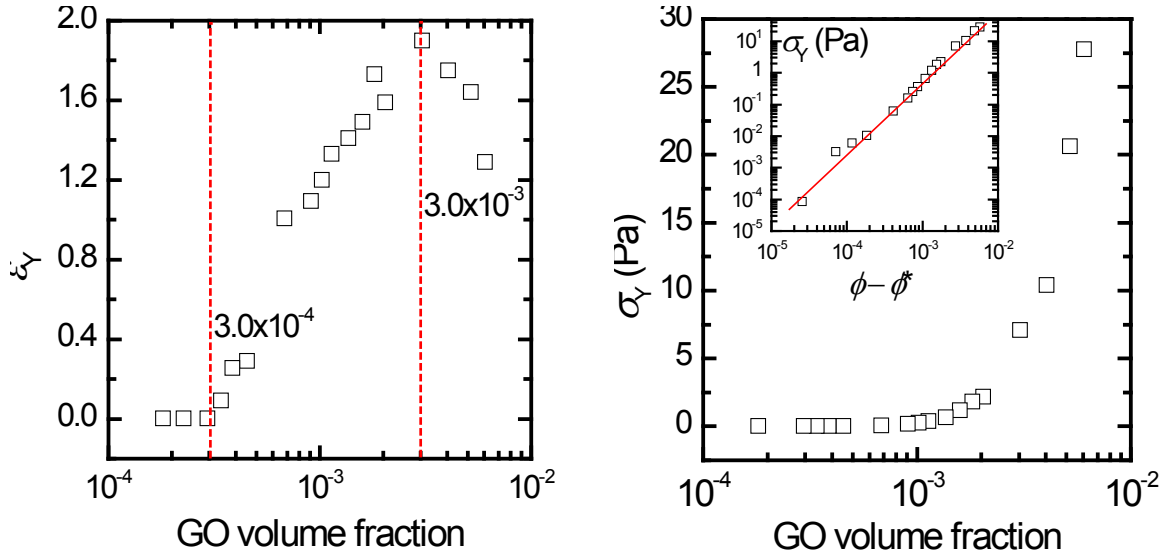

Fig. S4. (A) Yield strain vs GO volume fraction as shown in the previous Fig.. The red dotted lines indicate $\phi \sim 3.0\times10^{-4}$ after which yield strain begins to increase and $\phi \sim 3.0\times10^{-3}$ where yield strain starts to decrease. (B) Yield stress as shown in previous Fig. vs GO volume fraction. The inset shows σ_Y as a function of $\phi - \phi^*$. Here, $\sigma_Y \sim (\phi - \phi^*)^n$, where $\phi^* \sim 2.7 \times 10^{-4}$, and $n = 2.5$. Both ϕ^* and n are in very good agreement with parameters obtained for plateau storage modulus (Fig. 1). Of note, the storage moduli used to calculate σ_Y is not the same as those in Fig. 1. $\sigma_Y = G'_Y \varepsilon_Y$ where G'_Y is the storage modulus at yield point and ε_Y is yield strain.

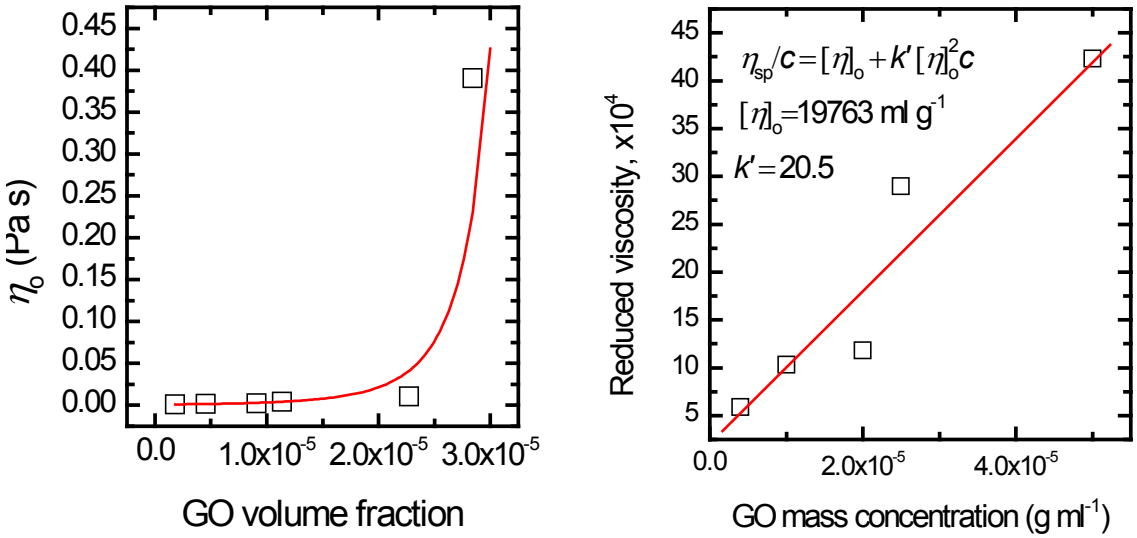

Fig. S5. (A) Viscosity of very dilute GO suspensions vs GO volume fraction. The red line is the best fit of: $\eta_o/\eta_w = (1-\phi/\phi_m)^{-\tau}$, where $\phi_m \approx 4.2\times10^{-5}$. From [Solid State Commun. 1984, 50 (11), 999-1002], the estimated diameter for a sheet ~ 1 nm thick is 22.4 – 44.8 µm. (B) Reduced viscosity $[\eta] = (\eta-\eta_s)/(\eta_s c)$ vs GO mass concentration c. From fitted linear line inherent viscosity is calculated $[\eta]_o$=19763 ml g^{-1}. Using a simplified Kuhn and Kuhn disk model the average GO sheets aspect ratio can be estimated from $[\eta]_o \approx \frac{32}{15\pi}(D/t)$. Estimated sheet diameter obtained using this model is ~ 29 µm.

Supplementary Tables

Table S1. Rheological characteristics of GO dispersions as function of GO concentration along with subsequent fabrication methods

Concentration range	LC Phase	Rheological characteristics					Electrostatic spraying	Ink-jet printing	Wet-spinning	Extrusion printing of 2D patterns	Extrusion printing of 3D architectures	Dry-Spinning
(mg ml-1)		Region	Viscosity by increasing the concentration	Viscoelastic behaviour								
				Long time scale (0.1Hz >)	Intermediate time scale (0.1Hz> >10 Hz)	small time scale (> 10 Hz)						
0.25 > C	Isotropic	Viscoelastic liquid	Negligible	G"> G'	G"> G'	G"> G'	suitable	not suitable	not suitable	not suitable	not suitable	not suitable
0.75> C ≥ 0.25	Biphasic	Transition state to viscoelastic soft solid	Increase to 16.5 Pa S^{-1} then decrease to 2.5 Pa S^{-1}	G"< G'	G"> G'	G"< G'	suitable	suitable	not suitable	not suitable	not suitable	not suitable
2.5 ≥ C ≥ 0.75	Nematic	Viscoelastic soft solid	Increase to 5 Pa S^{-1}	G"< G'	G"=G'	G"> G'	not suitable	suitable	suitable	not suitable	not suitable	not suitable
4.5 ≥ C > 2.5	Columnar	Viscoelastic gel	Increase to 67 Pa S^{-1}	G"< G'	G"< G'	G"> G'	not suitable	not suitable	suitable	suitable	not suitable	not suitable
C > 4.5	Columnar	Viscoelastic gel	Constant at around 70 Pa S^{-1} then increase up to 655 Pa S^{-1}	G"< G'	G"< G'	G"< G'	not suitable	not suitable	suitable	suitable	suitable	suitable

Author Contribution Statements

S.H.A. initiated and conceptualized the project. R.J. and S.H.A. synthesised graphene oxide. R.J. performed the initial rheological properties. R.J. initiated the idea of the correlation of processability and flow behaviour. S.N. conceived and conducted the rheological experiments, analysed the data and plotted the graphs. R.J. and R.A.G. were in charge of the fabrication methods. R.J. and S.H.A. performed POM analysis and characterized the liquid crystallinity. S.N. wrote the initial drafts of the manuscript. R.J. prepared the final Figures including schematics. S.N., R.J. and S.H.A. interpreted the data, discussed the results and performed final edits. S.H.A. wrote the final manuscript. G.G.W. oversaw all research phases and revised the manuscript in collaboration with all co-authors. P.P. assisted with the discussions on LC formation. G.G.W., K.K., P.C.I and G.M.S. are principle investigators of the supporting grants. All authors contributed to writing and revising the manuscript, and agreed on its final contents.

References

1 Hough, L. A., Islam, M. F., Janmey, P. A. & Yodh, A. G. Viscoelasticity of Single Wall Carbon Nanotube Suspensions. *Phys. Rev. Lett.* **93**, 168102, (2004).

2 Jalili, R. *et al.* On the Formation and Processability of Liquid Crystalline Dispersions of Graphene Oxide. Theory and Practice" to Materials Horizons. *Materials Horizons* Submitted, (2013).

3 Mourad, M. C. D. *et al.* Sol−Gel Transitions and Liquid Crystal Phase Transitions in Concentrated Aqueous Suspensions of Colloidal Gibbsite Platelets. *J. Phys. Chem. B* **113**, 11604-11613, (2009).

4 Zhou, Z. & Wu, X.-F. Graphene-beaded carbon nanofibers for use in supercapacitor electrodes: Synthesis and electrochemical characterization. *Journal of Power Sources* **222**, 410-416, (2013).

5 Kroon, M., Vos, W. L. & Wegdam, G. H. Structure and formation of a gel of colloidal disks. *Phys. Rev. E* **57**, 1962-1970, (1998).

6 Chien, C.-T. *et al.* Tunable Photoluminescence from Graphene Oxide. *Angew. Chem. Int. Ed.* **51**, 6662-6666, (2012).

7 Yousefi, N. *et al.* Self-alignment and high electrical conductivity of ultralarge graphene oxide-polyurethane nanocomposites. *J. Mater. Chem.* **22**, 12709-12717, (2012).

8 Eda, G. & Chhowalla, M. Graphene patchwork. *ACS Nano* **5**, 4265-4268, (2011).

9 Dong, Z. *et al.* Facile Fabrication of Light, Flexible and Multifunctional Graphene Fibers. *Adv. Mater.* **24**, 1856-1861, (2012).

10 El-Kady, M. F., Strong, V., Dubin, S. & Kaner, R. B. Laser Scribing of High-Performance and Flexible Graphene-Based Electrochemical Capacitors. *Science* **335**, 1326-1330, (2012).

11 Calvert, P. Inkjet Printing for Materials and Devices. *Chemistry of Materials* **13**, 3299-3305, (2001).

12 Derby, B. Inkjet Printing of Functional and Structural Materials: Fluid Property Requirements, Feature Stability, and Resolution. *Annu. Rev. Mater. Res.* **40**, 395-414, (2010).

13 Sollich, P., Lequeux, F., Hébraud, P. & Cates, M. E. Rheology of Soft Glassy Materials. *Phys. Rev. Lett.* **78**, 2020-2023, (1997).